

ANALYSIS OF DEFORMATION PROCESSES USING BLOCK-MATCHING TECHNIQUES

Alvaro Rodriguez¹, Carlos Fernandez-Lozano¹, Jose-Antonio Seoane¹, Juan R. Rabuñal¹
and Julian Dorado²

¹Information and Communications Technologies, University of A Coruña, Campus Elviña sn, 15007, A Coruña, Spain

²Centre of Technological Innovation in Construction and Civil Engineering, University of A Coruña,
Campus Elviña sn, 15007, A Coruña, Spain

Keywords: Computer Vision, Optical Flow, Deformation, Block-matching.

Abstract: Non rigid motion estimation is one of the main issues in computer vision. Its applications range from civil engineering or traffic systems to medical image analysis. The challenge consists in processing a sequence of images from of a physical body subjected to deformation processes and extracting its displacement field. In this paper, an iterative Block-Matching technique is proposed to measure displacements in deformable surfaces. This technique is based on successive interpolation and smoothing phases to calculate the dense displacement field of a body. The proposed technique was experimentally validated by studying the Yosemite sequence and it was tested in the analysis of strength test and biomedical images.

1 INTRODUCTION

The motion estimation in deformable surfaces has been an issue of continuous major interest in several areas ranging image diagnosis in medicine, structure analysis in civil engineering and others.

In a general formulation of the problem, it is necessary to estimate the motion in a scene in a time interval Δt . By analysing two frames; I and I' representing the states in the instants t and $t + \Delta t$.

Optical flow techniques are a field of computer vision born in the 80s (Horn and Schunk, 1981). They provide a flexible approach to extract the motion field of a scene.

A group of these techniques, the Block-Matching techniques, calculate the displacement from a pair of images, dividing the first one into small regions or blocks and finding the correspondence for each block in the second image using a search range.

Although the Block-Matching techniques are limited due to the size and shape of the blocks, they have been applied successfully in several fields such as civil engineering (Raffel et al. 2000) and in medical image analysis (Basarab et al. 2007). Currently it is one of the most robust methods for extracting the displacement field of a surface without reference points such as corners or edges.

Several contributions have been made to Block-

Matching techniques. The most important are the inclusion of pyramidal decomposition techniques to reduce computational cost and to avoid local minima (Amiaz et al. 2007), the use of Fourier Transforms (FTs) and subpixel estimators (Raffel et al. 2000) to increase accuracy.

More recently, the use iterative warping techniques have been proposed (Basarab et al. 2007 ; Raffel et al. 2007), some models to improve the performance with rotational displacements have been analysed (Ng et al. 2010) and new similarity metrics have been proposed (Grewenig et al. 2011).

2 PROPOSED TECHNIQUE

The technique proposed follows the main principles of any block matching technique. Dividing the image in non overlapping regular regions called blocks and solving the correspondence problem for each block in the next image.

The proposed algorithm calculates the motion vectors of the scene using an iterative represented in Fig.1. The main steps of the algorithm are the following.

1. The sequence of images is acquired with a digital camera or a similar device.

2. The image is downsampled with a standard pyramidal decomposition algorithm.
3. A similarity metric and a search algorithm are used to calculate the best discrete displacement.
4. The similarity values are used to perform a fitting to a 2D Gaussian function with the Levenberg-Marquardt technique to achieve a subpixel accuracy.
5. The obtained vectors are filtered and smoothed.
6. The optical Flow (formed by the vectors of displacement for each block) has been obtained.
7. The Optical Flow is processed with an interpolation algorithm, obtaining the displacements for each pixel of each block.
8. The blocks are deformed using the information of the displacement; a new interpolation step is required to obtain the new blocks from the image. The new blocks are used to improve the results from the previous iteration or to estimate the initial position of the blocks in the next frame.
9. If the last iteration has been performed, The Dense Deformation Field (the vectors of displacement for each pixel of the image) has been obtained.

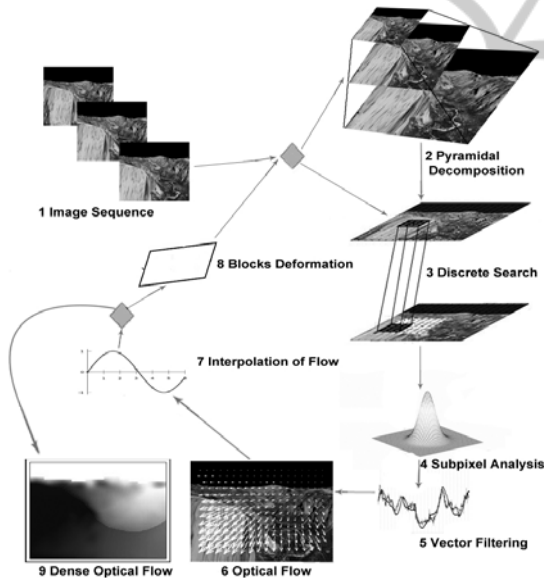


Figure 1: General scheme of the proposed algorithm.

2.1 Discrete Displacement

To measure the degree of correspondence for each block of I with another block from I' , the proposed algorithm uses the statistical similarity of the gray levels in both regions.

The original block is centered in the point (i, j) in the image I . After applying a displacement $d(i, j) = (x, y)$, this block will correspond with the region centered in (i', j') in I' . This is described in (1).

$$(i', j') = (i + x, j + y) \quad (1)$$

This approach is based on the assumption expressed in (2).

$$I(i, j) + NF = I'(i + x, j + y) \quad (2)$$

NF being a noise factor following a specific and unknown statistical distribution, I the original image and I' the deformed one.

To find the point (i', j') a set of candidate blocks will be defined in I' using a search range from (i, j) . Therefore, the objective will be to find the candidate region maximizing a similarity function with the original one.

In this work, the Pearson's correlation quotient (R) is used to that end (3).

$$R_{ij}(i', j') = \frac{\sum_N ((I(i, j) - \mu) \times (I'(i', j') - \mu'))}{\sqrt{\sum_N (I(i, j) - \mu)^2 \times \sum_N (I'(i', j') - \mu')^2}} \quad (3)$$

Where N is the size of the block, μ and μ' are the average intensity values of the blocks centered in $I(i, j)$ and $I'(i', j')$ respectively.

The chosen metric (R) has the advantages of being invariant to the average gray level and therefore it is robust in presence of some natural variability processes such as those present in common light sources.

2.2 Subpixel Accuracy

The accuracy of the technique presented so far is limited to the pixel level due to the digital nature of the images.

However, the correlation value itself contains some useful information, given that the values achieved in the pixels surrounding the best value will reflect one part of the displacement located between both pixels.

Thus, the correlation can be translated to a continuous space using a numerical fitting technique. Here, the two-dimensional Gaussian function defined in (4) has been used as a continuous model of the correlation values.

$$f(x, y) = \lambda \times e^{-\left[\frac{(x-\mu)^2}{2 \times \sigma^2} + \frac{(y-\mu)^2}{2 \times \sigma^2} \right]} \quad (4)$$

Being λ , μ_x , μ_y , σ_x and σ_y the parameters of the function. This parameters are calculated by performing a fitting using the Levenberg-Marquardt (LM) method as defined in (5).

$$\begin{aligned} (J_{n \times 5}^T \times J_{n \times 5} + d \times I_5) \times Inc_{5 \times 1} &= J_{n \times 5}^T \times E_{n \times 1} \\ J_{n \times 5} &= \begin{bmatrix} \frac{\partial f(x_1, y_1)}{\partial \lambda} & \dots & \frac{\partial f(x_n, y_n)}{\partial \lambda} \\ \dots & \dots & \dots \\ \frac{\partial f(x_1, y_1)}{\partial \sigma_y} & \dots & \frac{\partial f(x_n, y_n)}{\partial \sigma_y} \end{bmatrix}_{n \times 5} \end{aligned} \quad (5)$$

With $d \in N^+$, $d \neq 0$ adjusted for each algorithm iteration, E is the error matrix, J the Jacobian matrix of f and Inc the vector of increments for the next iteration.

The following initial estimation for the function parameters have been used: $\lambda = \max(R_{ij})$, $\mu x = 0$, $\mu y = 0$, $\sigma x = 2$ and $\sigma y = 2$.

The algorithm for updating d is shown in (6). According to it, the Residual Sum of Squares (RSS) is calculated from the error matrix (E), so that if the RSS decreases, the d value is fixed to a constant near to 0, so the algorithm gets close to the Gauss-Newton one; in other instances, the d value increases so that the algorithm behaves as a gradient descent method.

$$\begin{aligned} d^0 &= 1e-7 \\ \left\{ \begin{aligned} &((k-1) \geq kMax) \cup (d > dMax) \Rightarrow FINISH \\ &RSS^k < RSS^{k-1} \Rightarrow d^{k+1} = d^0, v = 2 \\ &RSS^k \geq RSS^{k-1} \Rightarrow d^{k+1} = d^k \times v, v = 2 \times v \end{aligned} \right. \end{aligned} \quad (6)$$

Where $kMax$ and $dMax$ can be adjusted by the user.

2.3 Vector Filtering

Once the displacement vectors have been calculated, a vector processing algorithm has been used to replace the anomalous vectors and to obtain a soft vector field. This is done in two steps:

1. First, the root mean square (RMS) of the neighbors of each vector is calculated. If the difference of this value with the estimated one is greater than a threshold set by the user, the vector is replaced by the RMS .
2. Finally, the vector field is smoothed with a bidimensional Gaussian filter. The default filter uses a 3×3 sized window.

2.4 Deformation of the Blocks

It should be noted that, if non-rigid displacements are considered the assumption expressed in (2) is generally false because neither rotation nor second order effects are included in the model.

Generally, it can be assumed that if the regions or blocks are small enough, then the second order

effects may be disregarded and strains can be calculated from the locally linear displacements in every region.

If deformations are considered, the objects in the scene start in an initial non-deformed stage and develop to a final deformed one. The same principle can be applied to blocks. They start with a regular rectangular shape and, using the information from the measured displacement, the shape of the block can be changed according to the deformations of the body in the scene.

Thus, using the vector field obtained in the previous iteration or from a previous frame of the scene, a dense displacement field is obtained by interpolating the motion vectors.

The dense field can be used to obtain the new positions of the pixels in the block and with this information a second interpolation step can be used to obtain the deformed block.

The deformed block is used to improve the measurement from the previous iteration or to predict the shape of the surface in the next frame.

In the presented work, bilinear and bicubic B-spline interpolation methods were used to interpolate the displacement field and the data of the block respectively.

3 EXPERIMENTAL RESULTS

3.1 Synthetic Images

The first assay was performed with synthetic images. In this experiment, the Yosemite synthetic sequence was used. This is a standard test for benchmarking optical flow algorithms. It was created by Lynn Quam (Heeger, 1987) and it was widely studied in different works (Austvoll, 2005).

Besides, this sequence is one of the best to perform an evaluation of a Block-Matching algorithm, since it contains a single surface with a complex motion, which is the kind of motion where the use of Block-Matching technique makes sense.

This experiment was performed analyzing the motion between consecutive frames, calculating the statistics of error according to the true ground data and using the metrics and methodologies published in (Scharstein et al. 2007). According to this, the error was calculated using the dense displacement field except a border region with a size of 10 pixels (7).

The obtained results were calculated using non-overlapped blocks of 15×15 pixels and 5 iterations.

An example of obtained results is shown in Fig. 2.

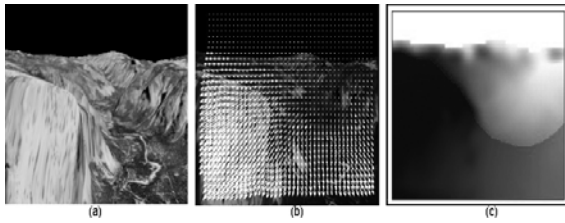


Figure 2: Yosemite experiment. (a) First frame (b) Last frame and motion vectors of the blocks. (c) Dense motion field (gray level represents the magnitude of the displacement).

Table 1 shows the comparative results with other block matching methods. The following techniques were used:

1. The DaVis system, from LA Vision (PIV, 2011). It is a block-matching based technique introduced in (Raffel et al. 2000) and enhanced in (Raffel et al. 2007). It has been widely used in publications and experiments in various fields (Deng et al. 2004).
2. The Block-Matching technique provided by the computer vision library OpenCv available at (OPENCV, 2011).

Table 1: Comparative results in the Yosemite sequence using Block-Matching algorithms.

Algorithm	Average Error	SSD Error
<i>This Work</i>	0.11	0.11
LaVision (Raffel et al. 2007)	0.26	0.26
OpenCv (OPENCV, 2011)	0.43	0.55

Table 2 shows the results obtained with the proposed technique compared with those obtained by the top 15 grayscale algorithms from the Middlebury Ranking.

Table 2: Comparative results in the Yosemite sequence using the top 10 grayscale algorithms of the Middlebury ranking. More results and references are available in [4]

Algorithm	Average Error	SSD Error
2D-CLG	0.10	0.10
<i>This Work</i>	0.11	0.11
GroupFlow	0.11	0.26
LocallyOriented	0.12	0.11
Ad-TV-NDC	0.12	0.14
Modified CLG	0.12	0.16
Dynamic MRF	0.13	0.14
F-TV-L1	0.13	0.14
Learning Flow	0.14	0.16
Adaptive	0.14	0.17
Nguyen	0.14	0.13

The proposed technique obtained much better results than the tested block matching technique and the second best results for grayscale optical flow algorithms in the Middlebury ranking.

3.2 Application Field: 2D Gel Images

In proteomics, to separate proteins obtained from a sample the two-dimensional electrophoresis is commonly used. After the proteins have been separated, each dark spot represents different kind of proteins present in the sample and its size depends on the amount of protein.

In a typical association study, images are compared in pairs to find differences in proteins of interest. For this purpose, it is necessary to find the spot correspondence in the images (Almansa et al. 2007).

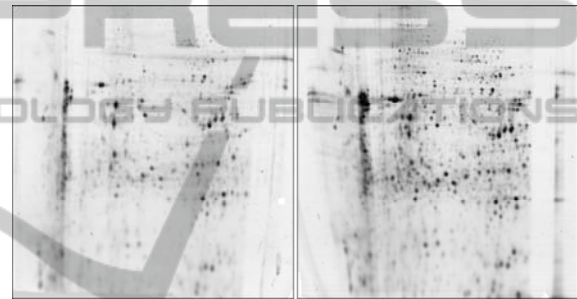


Figure 3: Example of two images in a 2D Gel experiment where it is necessary to find a spot correspondence.

The task is nowadays a bottleneck in the proteomics research (Voss and Haberl, 2000) and automatic analysis techniques can improve this process considerably.

The proposed technique has been used to match proteins of interest in 2D gel images. With this purpose blocks were defined using the position of the proteins in a reference frame and a simple analysis was performed avoiding the filtering and smoothing steps. This procedure is shown in Fig. 4.

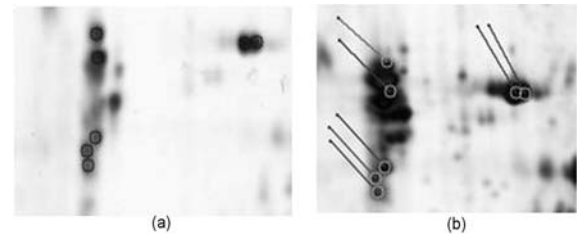


Figure 4: 2D Gel experiment. (a) Reference frame with marked proteins. (b) Protein displacement to achieve its final position in test image.

Table 3: Comparative results in proteomics.

Algorithm	Easy			Medium			Complex		
	n_{cor}	n_{inc}	%	n_{cor}	n_{inc}	%	n_{cor}	n_{inc}	%
<i>This Work</i>	204	4	98.1	154	4	97.5	46	9	83.7
Hybrid (Wrz et al. 2008)	203	5	97.6	153	5	96.8	-	-	-
Intensity (Wrz et al. 2008)	200	8	96.2	150	8	94.9	-	-	-
Hybrid (Rohr et al. 2004)	201	7	96.6	149	9	94.3	-	-	-
Intensity (Rohr et al. 2004)	187	21	89.9	137	21	86.7	-	-	-

The data used in the present work was built using images extracted from the Wolfson MIC Laboratory test sequences. In these data, every couple of images was assigned a complexity level according to the criterion of an expert.

Obtained results are shown in and summarized in Table 3. These results were compared with those published in (Rohr, 2004) and (Wrz et al. 2008) where the same data is used (although no results with high complexity images are provided).

Analysing the obtained results, it may be seen that the success rates obtained with biomedical images were higher than the rates reached by specific works using the same data.

3.3 Application Field: Strength Tests

Some of the main needs in Civil Engineering are to know the stress-strain response of materials used structures. For this purpose, strength tests are usually carried out by applying controlled loads or strains to a test model.

In, strength tests, information about the material's behavior is traditionally obtained using strain gauges or extensometers, these devices are expensive or non reusable and they must be physically linked to the material interfering with the experiment. Furthermore these devices provide only information about the length variation of the structure in a given point and in a single direction.

The proposed technique can be used to extract the full displacement field of the body without considering the points of interest or the main direction of deformation in the body.

In the next assay, a tensile test was performed with a cylindrical aluminum bar of 30cm length x 8mm diameter. The experiment was recorded with a video camera and the calibration technique proposed in (Zhang, 1999) was used to obtain measurements in a real scale. Fig.5 and Fig.6 illustrate how measurements were performed.

A traditional contact extensometer was used in this assay to compare the obtained results with those provided by traditional instrumentation.



Figure 5: 2D Gel experiment. (a) Reference frame with marked proteins. (b) Protein displacement to achieve its final position in test image.

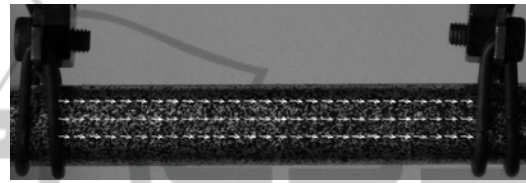


Figure 6: Displacement vectors estimated during the test and the extensometer attached to the material.

The vertical strain obtained (expressed in μ strains) for the section of the aluminum bar where the extensometer has been attached is shown in Fig.7.

Analysing the obtained results it may be seen that the proposed technique produces virtually identical results to those by extensometer.

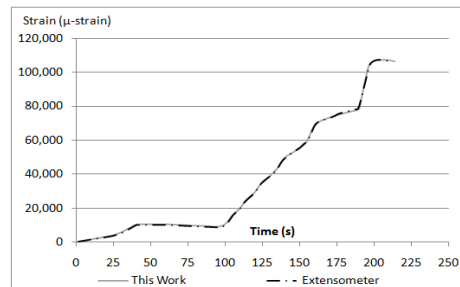


Figure 7: Graphic of the test with the aluminum. Strain obtained with the extensometer is shown together with the strain measured with the proposed technique.

4 CONCLUSIONS

The present paper introduces a new technique to analyze general deformable displacements in different surfaces without using displacement or deformation models.

The obtained results show that the proposed technique can retrieve the complete displacement field of a surface, obtaining accurate and robust results.

In the analysis of 2D gel images better results than specific works in the field were obtained and in the analysis of strength test the same precision as traditional devices was obtained avoiding the limitations of contact sensors.

ACKNOWLEDGEMENTS

This work was partially supported by the General Directorate of Research, Development and Innovation of the Xunta de Galicia (Ref. 08TMT005CT), grant (Ref.10SIN105004PR) funded by Xunta de Galicia and Consellería of Economy and Industry of the Xunta de Galicia (Ref. 10MDS014CT).

REFERENCES

- Almansa A, Gerschuni M, Pardo A and Preciozzi J: 2007. Processing of 2D Electrophoresis Gels *Iccv - Workshop on Computer Vision Applications for Developing Countries*.
- Amiaz T, Lubetzky E and Kiryati N: 2007. Coarse to overfine optical flow estimation. *Pattern Recognition*, 40(9):2494-1503.
- Austvoll I: 2005. A study of the yosemite sequence used as a test sequence for estimation of optical flow. *Lecture Notes in Computer Science*. 3540(2005):659-668.
- Baker S, Scharstein D and Lewis JP. Middlebury computer vision pages, an evaluation of optical flow algorithms. <http://vision.middlebury.edu/ow/eval>. (Accessed: 2011).
- Basarab, A, Aoudi W, Liebgott H, Vray D and Delachartre P. Parametric Deformable Block Matching for Ultrasound Imaging. *IEEE International conference on Image Processing*. (2007).
- Deng Z, Richmond MC, Guest GR and Mueller RP: 2004. Study of Fish Response Using Particle Image Velocimetry and High-Speed, High-Resolution Imaging, *Technical Report PNNL-14819*.
- Grewenig S, Zimmer S and Weickert J: 2011. Rotationally invariant similarity measures for nonlocal image denoising. *Journal of Visual Communication and Image Representation*. 22(2):117-130.
- Heeger D: 1987. Model for the extraction of image flow. *Journal of the Optical Society of America A: Optics, Image Science, and Vision* 4(1987):1455-1471.
- Horn BKP and Schunk BG: 1981. Determining optical flow. *Artificial Intelligence* 17:185-203.
- Ng KH, Po LM, Cheung KW and Wong KM: 2010. Block-Matching Translational and Rotational Motion Compensated Prediction Using Interpolated Reference Frame. *Journal on Advances in Signal Processing*.
- OPENCV. Open Source Computer Vision. <http://opencv.willowgarage.com> (Accessed: 2011).
- PIV. Particle image Velocimetry. <http://www.piv.de> (Accessed: 2011).
- Raffel M, Willert C and Kompenhans J: 2000. *Particle image velocimetry, a practical guide*. Springer, Berlin.
- Raffel M, Willert C and Kompenhans J: 2007. *Particle image velocimetry, a practical guide*, Second Edition. Springer, Berlin.
- Rohr K, Cathier P and Wrz S: 2004. Elastic registration of electrophoresis images using intensity information and point landmarks. *Pattern Recognition* 37:035-1048 .
- Scharstein D, Baker S, and Lewis JP: 2007. A database and evaluation methodology for Optical Flow. *ICCV*.
- Voss T and Haberl P: 2000. Observations on the reproducibility and matching efficiency of two-dimensional electrophoresis gels: consequences for comprehensive data analysis. *Electrophoresis* 21:3345-3350.
- Wrz S, Winz M and Rohr K: 2008. Geometric alignment of 2D gel electrophoresis images using physics-based elastic registration. *IEEE International Symposium on Biomedical Imaging: From Nano to Macro*.
- Zhang: 1999. Flexible Camera Calibration by Viewing a Plane From Unknown Orientations. *IEEE International Conference on Computer Vision*. 1: 666-673.